Transition Metal Dichalcogenides (WS_2 and MoS_2) Saturable Absorbers for Mode-Locked Erbium-Doped Fiber Lasers *

N. A. A. Kadir[1], E. I. Ismail[1], A. A. Latiff[2], H. Ahmad[2], H. Arof[1], S. W. Harun[1,2]**

[1]*Department of Electrical Engineering, Faculty of Engineering, University of Malaya, Kuala Lumpur 50603, Malaysia*
[2]*Photonics Research Center, University of Malaya, Kuala Lumpur 50603, Malaysia*

(Received 6 October 2016)

We demonstrate an ultrafast fiber laser based on transition metal dichalcogenide materials which are tungsten disulfide (WS_2) and molybdenum disulfide (MoS_2) as saturable absorber (SA). These materials are fabricated via a simple drop-casting method. By employing WS_2, we obtain a stable harmonic mode-locking at the threshold pump power of 184 mW, and the generated soliton pulse has 3.48 MHz of repetition rate. At the maximum pump power of 250 mW, we also obtain a small value of pulse duration, 2.43 ps with signal-to-noise ratio (SNR) of 57 dB. For MoS_2 SA, the pulse is generated at 105 mW pump power with repetition rate of 1.16 MHz. However, the pulse duration cannot be detected by the autocorrelator device as the pulse duration recorded is 468 ns, with the SNR value of 35 dB.

PACS: 42.55.Wd, 42.60.Da, 42.60.Fc, 42.70.−a DOI: 10.1088/0256-307X/34/1/014202

Passively mode-locked fiber lasers have received much attention for various applications, including optical frequency metrology, optical sensing, industrial material processing and terahertz generation.[1,2] They can be realized using nonlinear polarization rotation (NPR)[3] and semiconductor saturable absorber mirror (SESAM) techniques.[4] However, NPR has bulky construction and environmental sensitivity.[5,6] As for SESAM, it is expensive, narrow tuning range, and requires complex fabrication and packaging.[7] Later, carbon nanotube (CNT) and graphene have been extensively proposed in mode-locked fiber lasers as saturable absorber (SA) attributable to its remarkable properties including ease of fabrication, ultrafast recovery time and integration into fiber cavity.[8] Graphene is more preferable due to its low saturation threshold, ultrafast saturation recovery time and ultrabroad wavelength-independent saturable absorption range.[9] Nonetheless, graphene holds disadvantages, which are the difficulty to create an optical bandgap[4] and the weak modulation depth.[10]

Currently, other two-dimensional (2D) nanomaterials beyond graphene such as topological insulators (TIs),[11] black phosphorus,[12] and transition metal dichalcogenides (TMDs)[13] are also being studied and tested as an SA. Among these materials, TMD-layered materials have unique optical, mechanical and electronic properties.[14] Despite many fundamental studies of the structure and properties of TMDs including reports of monolayer[15] and few-layer crystals,[16] the lack of suitable processing and characterization techniques for such materials meant that their unique optical characteristics were not exploited for practical technologies.

Recent work has demonstrated wideband saturable absorption in few-layer molybdenum disulfide (MoS_2), suggesting that semiconducting TMDs could be a promising class of SA for short laser pulse generation.[17,18] More recently, other sulfide-based TMDs such as tungsten disulfide (WS_2) have emerged as candidate materials for future saturable absorbers. In this experiment, WS_2- and MoS_2-based SAs were developed using a simple drop and casting method for Q-switching applications. These SAs were developed by repeatedly dropping and drying the WS_2 and MoS_2 solution onto a fiber ferrule and thus they offer simplicity in fabrication compared with the composite film, in addition to allowing control over insertion loss. Here a simple and new approach to produce mode-locking pulses from erbium-doped fiber laser (EDFL) cavity is demonstrated using WS_2 and MoS_2 as the mode locker. By employing these SAs into a ring laser cavity, a stable mode locked EDFL could be obtained by controlling a cavity dispersion and nonlinearity.

These SAs are obtained from commercial WS_2 and MoS_2 pristine flake solution (purity ∼99%). According to the manufacturer, the WS_2 solution has a thickness and concentration of 1–4 layers and 26 mg/L, respectively. First, the WS_2 solution is repeatedly dropped and dried onto a fiber ferrule. The dried WS_2 is placed in the ring laser cavity as an SA for mode-locked pulse generation. The WS_2-based SA is employed to be generated in passive mode-locking in the EDFL cavity. The SA is used to realize nonlinear interaction of WS_2 nanomaterials with the propagating light in a laser cavity. This similar preparation process also goes for MoS_2-based SA. The thickness of MoS_2 solution used in this experiment is about 1–8 layers and the concentration is 18 mg/L.

Next, we investigate the strength of light absorption of the dried SAs through the I-scan (the balanced twin detector measurement system) technique. Based on I-scan, a power-dependent transmission technique was used to measure the nonlinear saturable ab-

*Supported by the University of Malaya under Grant No PG173-2015B.
**Corresponding author. Email: swharun@um.edu.my
© 2017 Chinese Physical Society and IOP Publishing Ltd

sorption of the WS_2 and MoS_2 SA. In this work, a stable self-produced passively mode-locked fiber laser with a repetition rate of 26 MHz and pulse duration of 600 fs operating at 1560 nm is used as the input pulse source. The output powers from both detectors are recorded as we gradually decrease the attenuation value. Figures 1(a) and 1(b) show the transmissions as they are plotted at various input intensities and its curve fitting. The power-dependent transmittance T is adapted by $T = A\exp[-\Delta T/(1 + I/I_{\rm sat})$, where A is the normalization constant, ΔT is the absolute modulation depth, I is the incident intensity, and $I_{\rm sat}$ is the saturation intensity. The saturation intensity can be determined from the half of its modulation depth value.[19] Based on Fig. 1(a), the saturable absorption and saturation intensity are obtained at 6.0% and 0. 18 MW/cm^2, respectively. Next, the nonlinear saturable absorption of the MoS_2 SA based on the same technique is measured. Figure 1(b) shows the nonlinear transmission curve where saturable absorption and saturation intensity are obtained at 3% and 0.06 MW/cm^2, respectively. These results indicate that the developed WS_2 and MoS_2 SAs are suitable for mode-locked application.

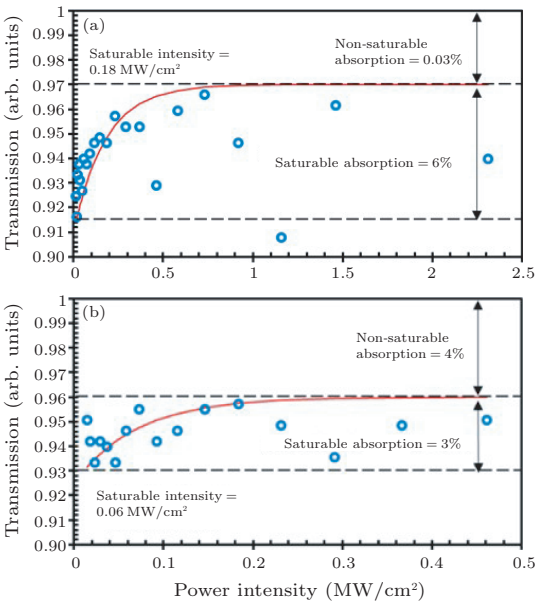

Fig. 1. Nonlinear saturable absorption profile of (a) WS_2 and (b) MoS_2 SAs.

Figure 2(a) shows the scanning electron microscopy (SEM) image of WS_2 flake solution, which has a lateral size in the range of 50–150 nm. The deposited WS_2 flakes solution are further characterized by the Raman spectroscopy, as depicted in Fig. 2(b). The characteristic bands at 350 and 420 cm^{-1} on the Raman spectrum are assigned to the in-plane (E_{2g}) and out-of-plane (A_{1g}) vibrational modes of WS_2 with frequency difference of 70 cm^{-1}. These presence modes agree well with those reported by Moa *et al.*[20] Figures 2(c) and 2(d) show the SEM image and the generated Raman spectrum, respectively, for the MoS_2 flakes solution, which is formed on the end surface of fiber ferrule. It has a lateral size in the range of 100–400 nm as shown in Fig. 2(c). The Raman spectrum exhibits two peaks at 381 cm^{-1} and 406 cm^{-1}, corresponding to the E^1_{2g} and A_{1g} modes, respectively. These peaks are separated from each other by 25 cm^{-1}, which is similar to the other reports.[21,22] These SEM images and Raman spectra are important to confirm the existence of WS_2 and MoS_2 element in the obtained solution.

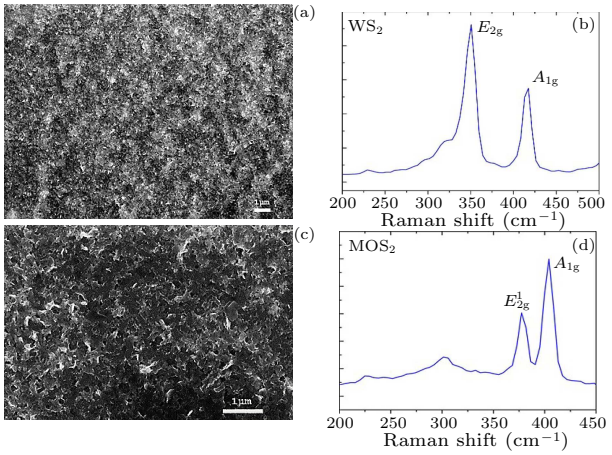

Fig. 2. Characteristics of the flakes solution before drying onto the end surface of the ferrule; WS_2: (a) SEM image and (b) Raman spectrum; MoS_2: (c) SEM image and (d) Raman spectrum.

Figure 3 presents the laser configuration of the laser setup, where the cavity consists of a 2.4 m EDF, a polarization-independent isolator, a WDM, an SA and a 90:10 coupler. The erbium-doped fiber has a concentration of 2000 ppm, absorption of 24 dB/m at 1550 nm and numerical aperture of 0.24. The isolator prevents backwards light propagation in the cavity. By using a 350-MHz oscilloscope together with a 1.3 GHz InGaAs photo-detector, the 10% laser output from the coupler is simultaneously monitored using an optical spectrum analyzer and a radio-frequency spectrum analyzer (RFSA).

An additional standard single mode fiber (SMF) of length 195 m is combined into the cavity to tailor the total group velocity dispersion (GVD) as well as to increase the nonlinearity effect so that mode-locking output pulse can be achieved. The ring cavity has total length of 204 m consisting of 2.4 m EDF and 201.6 m SMF, with group velocity dispersion (GVD) of 27.6, and -21.7 ps^2/km, respectively. The cavity runs in anomalous fiber dispersion of -4.44 ps^2, thus the soliton spectrum tends to be generated in the fiber laser. The pulse width of the mode-locked laser is recorded using an autocorrelator.

With the addition of SMF, the perfect match between the GVD and nonlinearity effect inside the ring cavity allows the generation of a stable mode-locking pulse. The stable self-starting mode-locking begins when the pump power reaches 184 mW. Figure 4(a) shows the output spectrum at the maximum pump power of 250 mW. The 3 dB spectral bandwidth is about 1.1 nm. At the power 250 mW, the spectrum shows

the soliton pulse in the sideband indicated that anomalous dispersion and nonlinearity occurs in the ring cavity. Inter-correlation between dispersion and nonlinearity in the ring cavity produces a good generation of soliton pulses. The stable self-starting mode-locking could be initiated without the polarization state in maintaining the stability of the soliton pulses, which means that the mode-locked pulses is independent of polarization, no polarization controller is required to control the polarization. The laser operates at the central wavelength of 1562 nm. In addition, to generate the stable mode-locked pulse without using PC to control the polarization state is quite hard. Figure 4(b) shows the average output power and pulse energy as a function of the pump power. It is observed that the output power and the pulse energy linearly increase with the pump power. The slope efficiency is relatively calculated about 2.51%. At the pump power of 250 mW, the pulse energy that can be obtained is 2.12 nJ. Figure 4(c) shows the oscilloscope pulse train at 250 mW pump power. The pulse train shows that a stable mode-locked pulse is uniform and not distinct in amplitude in each envelope spectrum with repetition rate of 3.48 MHz, which is consistent with the cavity round trip time. Due to the resolution limitation of the oscilloscope, the autocorrelator is employed to measure a pulse duration. Figure 4(d) shows the autocorrelation trace at the pump power 250 mW. By applying sech^2 fitting, the pulse duration at its FWHM is measured to be 2.43 ps. The autocorrelation trace reveals that the experimental data follows the sech^2 fitting closely. Then, our time-bandwidth product (TBP) is relatively about 0.328, which is slightly above the TBP of 0.315 in sech^2 pulse profile. In addition, the signal-to-noise ratio (SNR) of the fundamental peak to the pedestal extension is estimated as 57 dB in Fig. 4(e), which shows the stability of the pulse. The high repetition rate is achieved and shows that WS_2 works well in the EDFL ring cavity.

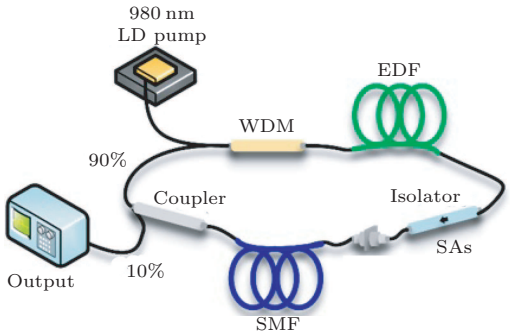

Fig. 3. Configuration of passively mode-locked EDFL based on WS_2 (or MoS_2) SA.

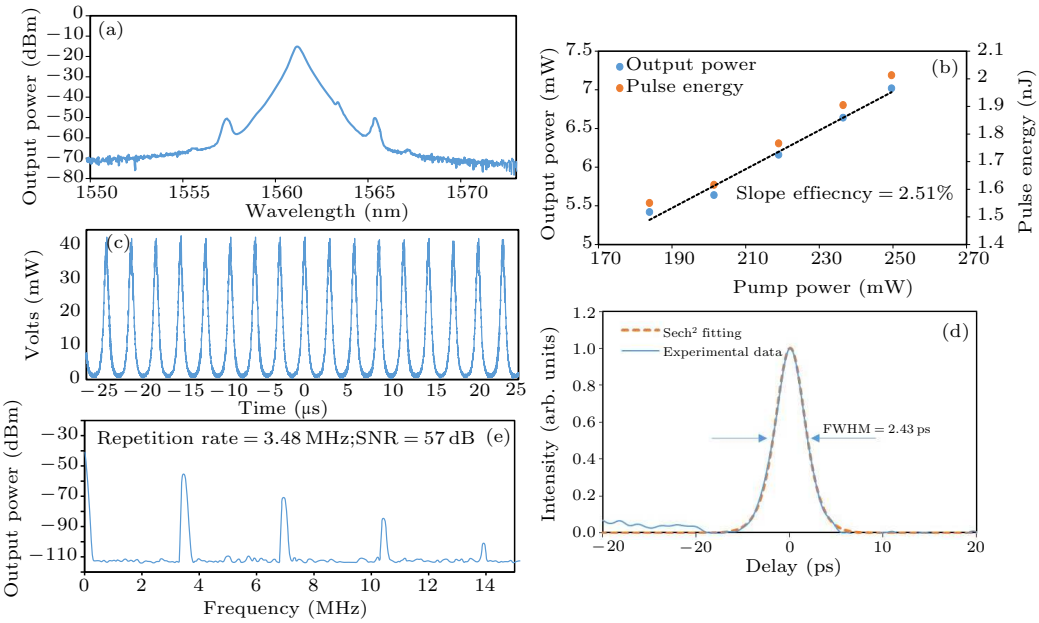

Fig. 4. Performances of WS_2-based mode-locked EDFL. (a) Output spectrum, (b) output power and pulse energy, (c) oscilloscope trace, (d) autocorrelation trace with sech^2 fitting curve, and (e) rf spectrum.

Next, the WS_2 solution will be replaced with MoS_2 solution and passive mode lock is demonstrated. A stable and self-starting mode-locked lasing begins when the power pump reaches 105 mW. Figure 5(a) shows the output spectrum of the mode-locked EDFL when the pump power reaches 140 mW. As seen in the figure, the laser operates approximately at the central wavelength 1566 nm. The spectral wavelength is broadening as the pump power increases due to the self-phase modulation effect in the ring cavity. With the incorporation of SA, the central wavelength is slightly shorter due to the loss in the ring cavity. Figure 5(b) shows the output power and pump energy when employing MoS_2 inside the laser cavity. The output power and pulse energy will increase directly proportional to the pump power. The output power increases from 6.7 mW to 9.17 mW while the pulse energy increases from 6.69 nJ to 9.13 nJ. We can obtain that the pulse energy could be improved as we increase the pump power threshold. In Fig. 5(c), the oscilloscope

pulse train at the maximum pump power of 140 mW is recorded. The pulse train shows a stable mode-locked pulse uniform and not distinct in amplitude in each envelope spectrum. As the pump power increases, the amplitude of the pulse also increases and narrows the pulse duration. The pulse starts to distort and become unstable when the pump power reaches above 140 mW and the pulses disappear with further increase of the pump power. The enlarged single pulse envelope in Fig. 5(d) indicates that the pulse duration is about 468 ns. By observing Fig. 5(e), our MoS_2-based mode-locked fiber laser which produces a stable pulse with SNR at maximum repetition rate of 1.004 MHz can be obtained to be about 35 dB.

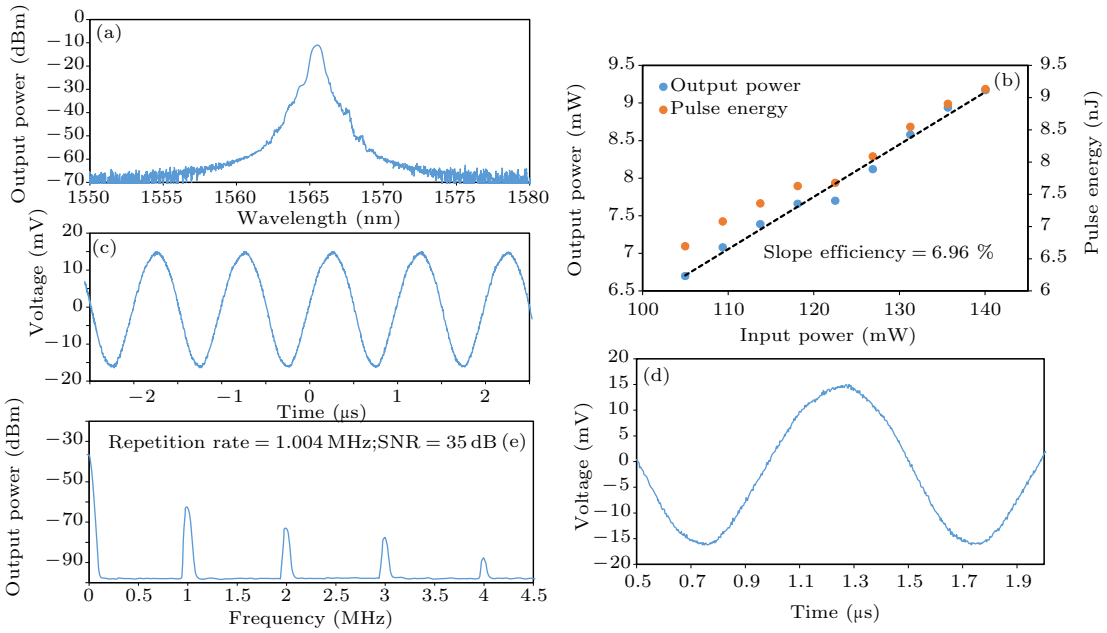

Fig. 5. Performances of MoS_2 based mode-locked EDFL. (a) Output spectrum, (b) output power and pulse energy, (c) oscilloscope trace, (d) single pulse envelope, and (e) rf spectrum.

In summary, passive mode-locked EDFLs based on the newly developed WS_2 and MoS_2 SA are experimentally demonstrated, with the total cavity length 204 m using a 2.4-m-long EDF as a gain medium operating in anomalous fiber dispersion of $-4.44\,ps^2$. With a WS_2 SA, a stable 2.43 ps soliton pulse operating at 1562 nm wavelength with the third harmonic repetition rate of 3.48 MHz is successfully obtained. Mode-locked pulse is realized at the threshold pump power of 184 mW with calculated maximum pulse energy as 2.0 nJ at the pump power of 249.6 mW, respectively. Furthermore, the fabricated MoS_2 SA can also work steadily at the mode-locked state with the pump power range of 105–140 mW. The MoS_2-based EDFL operates at 1566 nm with the fundamental frequency of 1.004 MHz and pulse width of 468 ns. Compared with the WS_2-based laser, this laser produces a higher pulse energy of 9.13 nJ. These results show that both WS_2 and MoS_2 SAs are simple, indicating low-insertion-loss, low-cost and ultrafast saturable absorption device for ultrafast photonic applications. Various applications may benefit from the ultrafast nonlinear features of these TMD materials.

References

[1] Oktem B et al 2010 *Nat. Photon.* **4** 307
[2] Keller U 2003 *Nature* **424** 831
[3] Wu J et al 2006 *Phys. Rev.* E **74** 046605
[4] Yan P et al 2015 *Sci. Rep.* **5** 12587
[5] Liu W et al 2016 *Photon. Res.* **4** 111
[6] Luo Z et al 2014 *IEEE J. Sel. Top. Quantum Electron.* **20** 1
[7] Huang S H et al 2012 *IEEE 21st Annual Wireless and Optical Communications Conference (WOCC)* p 178
[8] Kieu K and Wise F 2009 *IEEE Photon. Technol. Lett.: A Publication IEEE Laser Electro-Opt. Soc.* **21** 128
[9] Li H P et al 2014 *Chin. Phys.* B **23** 024209
[10] Zhang Y et al 2009 *Nature* **459** 820
[11] Yu Z et al 2014 *Opt. Express* **22** 11508
[12] Ismail E et al 2016 *RSC Adv.* **6** 72692
[13] Al-Masoodi A et al 2016 *Chin. Phys. Lett.* **33** 054206
[14] Komsa H P and Krasheninnikov A V 2013 *Phys. Rev.* B **88** 085318
[15] Chhowalla M et al 2013 *Nat. Chem.* **5** 263
[16] Lv R et al 2015 *Acc. Chem. Res.* **48** 56
[17] Woodward R et al 2015 *Photon. Res.* **3** A30
[18] Woodward R et al 2015 *Opt. Express* **23** 20051
[19] Jeon J et al 2015 *J. Opt. Soc. Am.* B **32** 31
[20] Mao D et al 2015 *Sci. Rep.* **5** 7965
[21] Yim C, O'Brien M et al 2014 *Appl. Phys. Lett.* **104** 103114
[22] Li H et al 2012 *Adv. Funct. Mater.* **22** 1385